On-chip spectrophotometry for bioanalysis using microring resonators

Arthur Nitkowski,[1,*] Antje Baeumner,[2] and Michal Lipson[1,3]

[1]*School of Electrical and Computer Engineering, Cornell University, Ithaca, NY 14853, USA*
[2]*Department of Biological and Environmental Engineering, Cornell University, Ithaca, NY 14853, USA*
[3]*Kavli Institute at Cornell for Nanoscale Science, Cornell University, Ithaca, NY 14853, USA*
**nitkowski@cornell.edu*

Abstract: We measure optical absorption in color-producing enzymatic reactions for biochemical analysis with a microscale optofluidic device. Cavity-enhanced laser spectrophotometry is performed on analytes within a microfluidic channel at visible wavelengths with silicon nitride microring resonators of 100 μm radius and quality factor of ~180,000. The resonator transmission spectrum is analyzed to determine optical absorption with a detection limit of 0.12 cm^{-1}. The device can be used to detect the activity of individual enzymes in a few minutes within a 100 fL sensing volume. The high sensitivity, small footprint, and low analyte consumption make absorption-based microring resonators attractive for lab-on-a-chip applications.

OCIS codes: (130.6010) Sensors; (300.6550) Spectroscopy, visible; (170.010) Medical optics and biotechnology; (140.3948) Microcavity devices.

References and links

1. C. Monat, P. Domachuk, and B. J. Eggleton, "Integrated optofluidics: A new river of light," Nat. Photonics **1**(2), 106–114 (2007).
2. D. Erickson, S. Mandal, A. H. J. Yang, and B. Cordovez, "Nanobiosensors: optofluidic, electrical and mechanical approaches to biomolecular detection at the nanoscale," Microfluid Nanofluidics **4**(1-2), 33–52 (2008).
3. W. G. Yang, D. B. Conkey, B. Wu, D. L. Yin, A. R. Hawkins, and H. Schmidt, "Atomic spectroscopy on a chip," Nat. Photonics **1**(6), 331–335 (2007).
4. Y. Fainman, L. Lee, D. Psaltis, and C. Yang, *Optofluidics: Fundamentals, Devices, and Applications* (McGraw-Hill, Inc., 2010).
5. M. L. Adams, M. Enzelberger, S. Quake, and A. Scherer, "Microfluidic integration on detector arrays for absorption and fluorescence micro-spectrometers," Sens. Actuators A Phys. **104**(1), 25–31 (2003).
6. W. E. Groves, F. C. Davis, Jr., and B. H. Sells, "Spectrophotometric determination of microgram quantities of protein without nucleic acid interference," Anal. Biochem. **22**(2), 195–210 (1968).
7. A. Fleck, and H. N. Munro, "The precision of ultraviolet absorption measurements in the Schmidt-Thannhauser procedure for nucleic acid estimation," Biochim. Biophys. Acta **55**(5), 571–583 (1962).
8. T. Mosmann, "Rapid colorimetric assay for cellular growth and survival: application to proliferation and cytotoxicity assays," J. Immunol. Methods **65**(1-2), 55–63 (1983).
9. M. Manafi, W. Kneifel, and S. Bascomb, "Fluorogenic and chromogenic substrates used in bacterial diagnostics," Microbiol. Rev. **55**(3), 335–348 (1991).
10. V. M. Cooke, R. J. Miles, R. G. Price, and A. C. Richardson, "A novel chromogenic ester agar medium for detection of Salmonellae," Appl. Environ. Microbiol. **65**(2), 807–812 (1999).
11. E. Shah Hosseini, S. Yegnanarayanan, A. H. Atabaki, M. Soltani, and A. Adibi, "High quality planar silicon nitride microdisk resonators for integrated photonics in the visible wavelength range," Opt. Express **17**(17), 14543–14551 (2009).
12. A. Nitkowski, L. Chen, and M. Lipson, "Cavity-enhanced on-chip absorption spectroscopy using microring resonators," Opt. Express **16**(16), 11930–11936 (2008).
13. J. Hu, N. Carlie, L. Petit, A. Agarwal, K. Richardson, and L. C. Kimerling, "Cavity-Enhanced IR Absorption in Planar Chalcogenide Glass Microdisk Resonators: Experiment and Analysis," J. Lightwave Technol. **27**(23), 5240–5245 (2009).
14. A. M. Armani, and K. J. Vahala, "Heavy water detection using ultra-high-Q microcavities," Opt. Lett. **31**(12), 1896–1898 (2006).
15. A. Waggoner, "Fluorescent labels for proteomics and genomics," Curr. Opin. Chem. Biol. **10**(1), 62–66 (2006).

#138424 - $15.00 USD Received 18 Nov 2010; revised 23 Dec 2010; accepted 27 Dec 2010; published 5 Jan 2011

16. J. R. Crowther, "ELISA. Theory and practice," Methods Mol. Biol. **42**, 1–218 (1995).
17. M. M. Mesulam, "Tetramethyl benzidine for horseradish peroxidase neurohistochemistry: a non-carcinogenic blue reaction product with superior sensitivity for visualizing neural afferents and efferents," J. Histochem. Cytochem. **26**(2), 106–117 (1978).
18. R. W. Boyd, and J. E. Heebner, "Sensitive disk resonator photonic biosensor," Appl. Opt. **40**(31), 5742–5747 (2001).
19. N. Jokerst, M. Royal, S. Palit, L. Luan, S. Dhar, and T. Tyler, "Chip scale integrated microresonator sensing systems," J Biophotonics **2**(4), 212–226 (2009).
20. C. A. Barrios, K. B. Gylfason, B. Sánchez, A. Griol, H. Sohlström, M. Holgado, and R. Casquel, "Slot-waveguide biochemical sensor," Opt. Lett. **32**(21), 3080–3082 (2007).
21. E. Krioukov, D. J. W. Klunder, A. Driessen, J. Greve, and C. Otto, "Sensor based on an integrated optical microcavity," Opt. Lett. **27**(7), 512–514 (2002).
22. A. Yariv, "Universal relations for coupling of optical power between microresonators and dielectric waveguides," Electron. Lett. **36**(4), 321–322 (2000).
23. A. Gondarenko, J. S. Levy, and M. Lipson, "High confinement micron-scale silicon nitride high Q ring resonator," Opt. Express **17**(14), 11366–11370 (2009).
24. J. N. Lee, C. Park, and G. M. Whitesides, "Solvent compatibility of poly(dimethylsiloxane)-based microfluidic devices," Anal. Chem. **75**(23), 6544–6554 (2003).
25. P. Heimala, P. Katila, J. Aarnio, and A. Heinamaki, "Thermally tunable integrated optical ring resonator with poly-Si thermistor," J. Lightwave Technol. **14**(10), 2260–2267 (1996).
26. D. M. Rissin, C. W. Kan, T. G. Campbell, S. C. Howes, D. R. Fournier, L. Song, T. Piech, P. P. Patel, L. Chang, A. J. Rivnak, E. P. Ferrell, J. D. Randall, G. K. Provuncher, D. R. Walt, and D. C. Duffy, "Single-molecule enzyme-linked immunosorbent assay detects serum proteins at subfemtomolar concentrations," Nat. Biotechnol. **28**(6), 595–599 (2010).

Introduction

The ability to perform spectroscopic measurements on-chip by combining microfluidic and nanophotonic capabilities would enable miniaturized, low-cost, fully automated, and massively parallel devices for lab-on-a-chip applications [1–5]. Many biomedical applications could benefit from an on-chip spectrophotometry tool such as the quantification of DNA/RNA/protein samples [6,7] and the analysis of colorimetric assays [8]. Also, current methods of bacteria detection include growing bacteria on selective and identifying media such as chromogenic agars [9]. These media change color as enzymes produced by the bacteria convert substrate molecules in the nutrient agar into a colored visible product. However, this method requires an incubation period of many hours to several days [10] in order for the color change to be strong enough for it to be identifiable by the naked eye or a microscope. We demonstrate here a platform that can, in principle, detect minuscule color changes produced by individual enzymes in a manner of minutes and therefore can be used in rapid chromogenic-based assays.

The platform is based on microring resonators for ultrasensitive absorption measurements in the visible regime [11]. These microcavities have been shown to be effective sensors for performing absorption spectroscopy on nanoliter volumes of fluids in the infrared regime [12–14] for chemical analysis. Here we show on-chip spectroscopic measurements of enzyme-produced absorption at visible wavelengths where nearly all biologically relevant chromophores and fluorophores have spectral features [15]. The microring resonators detect the color change that is produced by the conversion of a substrate molecule into a colored product by an enzyme commonly used in enzyme-linked immunosorbent assays (ELISA). ELISA is a powerful biochemical technique used to detect the presence of antibodies and antigens (such as proteins, clinical markers, pathogens, toxins, etc) in a sample [16]. The substrate molecule used often for these experiments is tetramethyl benzidine (TMB) which turns blue by the action of the enzyme horseradish peroxidase (HRP) [17]. In one example of an ELISA, HRP is conjugated to an antibody which is used to determine the presence of a target antigen. After binding to the antigen and the addition of the TMB substrate, the chromogenic reaction products can then be quantified at 650 nm which is the designed wavelength of operation for our device.

The principle of operation relies on the cavity enhancement of light in a microring resonator to detect changes in its local environment [18], as shown in Fig. 1a. Light is coupled

#138424 - $15.00 USD Received 18 Nov 2010; revised 23 Dec 2010; accepted 27 Dec 2010; published 5 Jan 2011

into the bus waveguide and a small fraction of light evanescently couples to the microring cavity. Light with a wavelength which fits an integral number of times within the ring circumference builds up due to constructive interference. In this way, light can circulate around the ring many times resulting in an effective path length that is orders of magnitude greater than the ring circumference. Due to this cavity enhancement, the ring is very sensitive to any changes in or around the waveguide since the effect of any perturbation is multiplied by the number of round trips that light undertakes. Since the evanescent field of the waveguide mode extends into the analyte (see Fig. 1b), any optical absorption present in the analyte within the evanescent field of the microring will alter the resonance transmission characteristics of the device. Note that this technique is fundamentally different from refractive index based sensors which measure a shift in the resonance position due to a binding event [19–21]. Refractive index sensors can be compromised by binding of non-target molecules as well as thermal fluctuations which can also shift the resonant wavelength. In contrast, by using absorption as the measurement metric, the sensor presented here provides reaction specific spectral information which does not suffer from the above drawbacks.

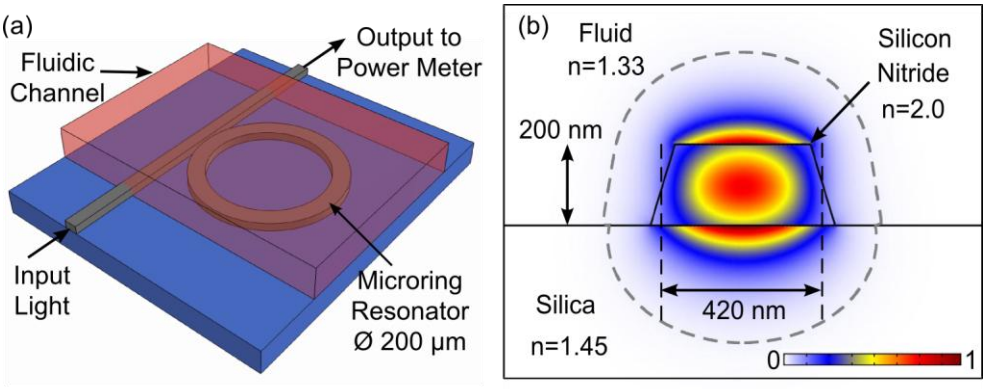

Fig. 1. (a) Device design for a microring resonator covered by a microfluidic channel. The microring enhances the interaction length between the cladding fluid and the evanescent field of the guided mode. (b). Numerical simulation of the $|\vec{E}|^2$ profile of the TM mode in a silicon nitride waveguide at a wavelength of 650 nm and covered with an aqueous solution. The dashed line is the contour at which the field decays to 1% its maximum value.

Materials and methods

The relations describing the optical power coupling from a dielectric waveguide to a ring resonator are well known [22]. The power transmission at the output of the waveguide is given by:

$$T(\theta) = \frac{a^2 + |t|^2 - 2a|t|\cos\theta}{1 + a^2|t|^2 - 2a|t|\cos\theta} \tag{1}$$

where a is the field attenuation coefficient which quantifies the sidewall scattering, bending loss, and most importantly the absorption induced by the enzymatic reaction. The field attenuation coefficient is related to the more familiar power attenuation coefficient, α, which is also called the absorption coefficient, by the relation $\alpha = -2\ln a/L$. The field transmission coefficient, t, accounts for coupling losses between the ring and waveguide, and θ is the phase shift per round trip. The phase shift can be expressed in terms of the light frequency, ω, circumference of the ring, L, and the effective index n_{eff} as $\theta = \omega L n_{eff}/c$. Since the evanescent field of the mode in the ring extends into the analyte material, any optical absorption in the material will increase the round trip propagation losses and decrease the

#138424 - $15.00 USD Received 18 Nov 2010; revised 23 Dec 2010; accepted 27 Dec 2010; published 5 Jan 2011

value of the measured field attenuation coefficient. The absorption in the analyte can be related to the absorption in the ring by numerically calculating the mode overlap of the field with the analyte. For our case this mode overlap, also called the confinement factor, is Γ = 0.22. Figure 2 shows how the resonance curve, described by Eq. (1) changes as the absorption in the cladding material increases. The resonance linewidth broadens and the extinction ratio decreases as losses increase. Also shown in Fig. 2 are the curves fit to each transmission spectrum, from which we extract the ring's attenuation coefficient and determine the loss contribution due to the analyte.

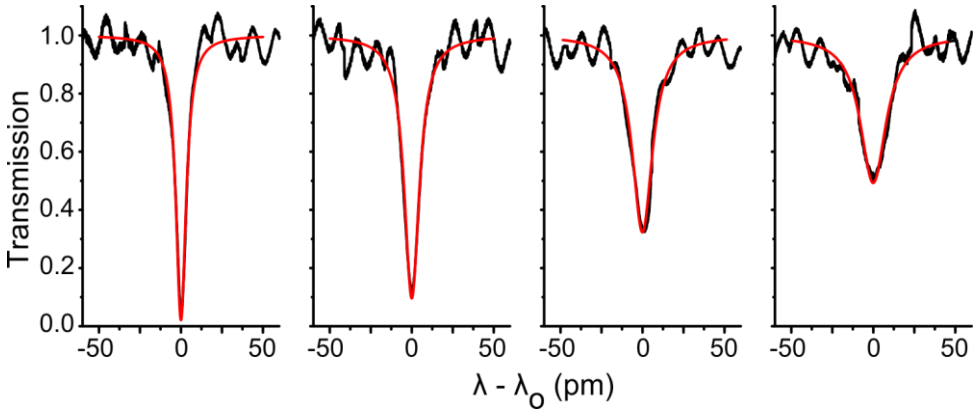

Fig. 2. Experimentally measured transmission spectrum of a microring resonator (black line) with fluid analytes of increasing absorbance (left to right) showing the change in extinction ratio and linewidth as the resonator loss increases. The data was fit (red line) using Eq. (1) to extract the absorption coefficient of the cladding fluids.

The nanophotonic devices are fabricated using standard microlithography techniques. Four microns of thermal oxide was first grown on top of a silicon wafer. Stoichiometric silicon nitride was deposited, 200 nm thick, with low pressure chemical vapor deposition (LPCVD). An electron beam resist (MaN 2403) was spun on top of the wafer followed by a conductive layer (ESPACER). The ring resonators and bus waveguides were patterned using a JEOL 9300 E-beam system. After development to remove unexposed resist, the wafer underwent a post exposure bake for 5 min at 145 °C to reflow the resist surface to minimize roughness. The devices were then etched using inductively coupled reactive ion etching (ICP RIE) with a CHF_3/O_2 process chemistry. Non-vertical etching led to a sidewall angle of approximately 15 degrees resulting in a trapezoidal waveguide cross section as shown in Fig. 1b. The devices were annealed at 1200 °C for 120 minutes at atmospheric pressure. The devices were cut from the wafer with a dicing saw and the end facets polished. A lift-off process is used to mask a 250 µm channel perpendicular to the waveguide while the rest of the waveguide is clad with 3.5 µm of evaporated silicon oxide. Further details on the waveguide fabrication can be found at [23] where a similar process was used with demonstrated waveguide propagation losses of 0.1 dB/cm in the near infrared.

Microfluidic capabilities are integrated with the photonics using polydimethylsiloxane (PDMS) soft lithography processes [24]. A 30 µm tall by 300 µm wide channel mold is patterned with SU8 channels on a silicon wafer. PDMS is poured over the channel mold, allowed to cure, and then inlet holes are punched to access the channels. The microfluidic slab is then aligned on top of the unclad portion of the waveguides using a contact aligner.

The device performance is measured with various fluids which are prepared by controlling enzyme concentration. First, 5 mg of horseradish peroxidase powder (Thermo Scientific) was dissolved into 5 mL of deionized water. This solution was twice diluted by 100 times to generate a solution with concentration of 100 ng/mL. Separately in a 96-well plate, 100 µL of the substrate TMB (KPL SureBlue Reserve) was added to 6 wells. Different amounts of the

#138424 - $15.00 USD Received 18 Nov 2010; revised 23 Dec 2010; accepted 27 Dec 2010; published 5 Jan 2011

HRP enzyme solution were then added to the 6 substrate-containing wells to produce a final enzyme concentration in the wells of 6, 4, 2, 1, 0.5, and 0 ng/mL. Upon addition of the enzyme solution, the color of the fluid in the wells began to produce a blue tint due to the HRP catalyzed conversion of the TMB substrate into a colored product. The color was allowed to develop for 5 minutes and then a stopping solution (KPL TMB BlueSTOP) was added. The stopping solution prevents further enzyme activity and the absorbance values of the fluid in the wells maintain a constant level which allows reliable measurements to be performed on the samples over an extended time period. The absorbance values of the well-mixed fluids were measured in the 96-well plate with a commercial spectrophotometer (Spectramax Plus 384) and the absorption spectrum is shown in Fig. 3a. The fluids are then individually measured by our optofluidic device.

Results and discussion

The performance of the device is characterized by measuring the ring resonator response to fluids with a range of absorbance values, as shown in Fig. 2. For each fluid with different enzyme concentration, the ring transmission is experimentally measured using a tunable laser which sweeps the frequency of light through a resonance and records the transmitted optical power. The light source is a 1 mW fiber coupled external cavity diode laser (Sacher Lasertechnik TEC 530) with wavelength range of 640 nm – 653 nm. Note that for future applications the transmission spectrum can be measured in principle using a single light source and a heater to temperature tune the resonances [25]. Light with wavelength of 650 nm is coupled into the waveguides using a polarization maintaining optical fiber that is positioned into physical contact with the polished waveguide end facet. The waveguide output is collected with a high numerical aperture microscope objective and sent through a polarizer to ensure measurement of the proper polarization. The polarized light is split to both a wavemeter (Advantest) and power meter to simultaneously record power and frequency. The intrinsic ring performance is determined by measuring a ring resonance without any absorption caused by the addition of HRP enzymes. The extracted field attenuation coefficient is 0.965 ± 0.004 which corresponds to an intrinsic quality factor of ~180,000 and a waveguide propagation loss of 4.9 dB/cm.

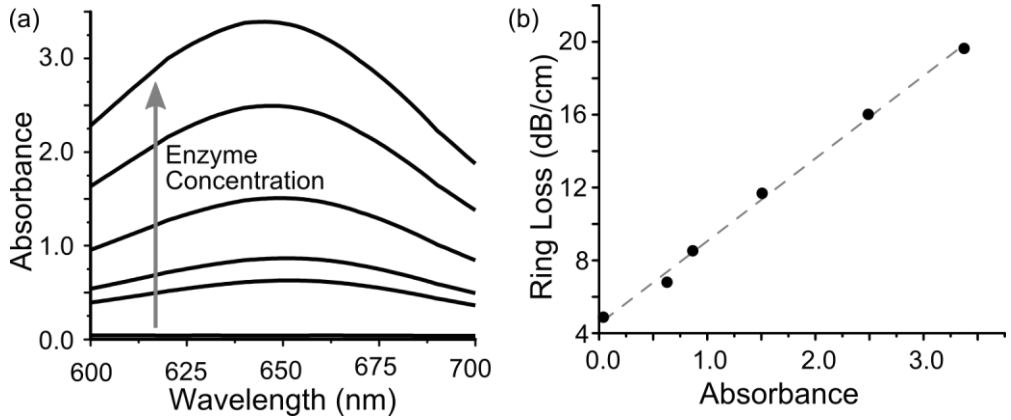

Fig. 3. (a) Fluid absorbance measured with a commercial spectrophotometer with enzyme concentrations 6, 4, 2, 1, 0.5, and 0 ng/mL. (b) The resulting ring propagation losses as a function of the absorbance when the same fluids are measured with a microring resonator at a wavelength of 650 nm.

We show a linear relationship between the absorbance of the analyte fluid (as measured from a commercial spectrophotometer) and the total waveguide propagation loss in the ring (see Fig. 3b), indicating the ability of the device to accurately determine the absorbance of an analyte within the range commonly measured (0-4 AU) with spectrophotometers. The

#138424 - $15.00 USD Received 18 Nov 2010; revised 23 Dec 2010; accepted 27 Dec 2010; published 5 Jan 2011

absorbance values for the fluid are normalized by the spectrophotometer to a path length of 1 cm. The limit of detection is determined by making multiple measurements and the resulting standard deviation is considered the noise floor of our experiment. After 10 consecutive scans on the same resonance, the deviation in the extracted field attenuation coefficient is $\sigma = 0.0038$ which is less than 0.4% its nominal value of $a = 0.965$. This deviation in the ring performance metric corresponds to a detection limit of 0.12 cm^{-1} in the fluid absorption coefficient. The noise floor is currently limited by the laser intensity fluctuations due to mode-hopping during wavelength tuning which could be reduced by either using a different light source or using temperature tuning for spectral measurements.

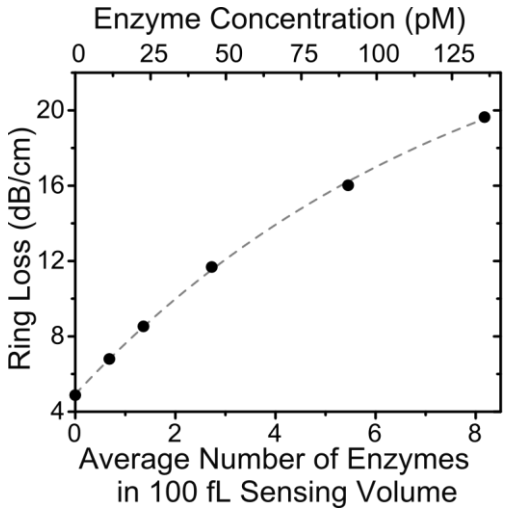

Fig. 4. Ring propagation loss as a function of both enzyme concentration and the number of enzymes within the sensing volume of the microring resonator (~100 fL).

Based on the data presented, we calculate a sensitivity capable of measuring the products of individual enzyme molecules after only a few minutes of acitivity. The best possible sensitivity of the device can be determined by considering the concentration of enzymes within the sensing volume of the ring resonator. The microfluidic channel covering the ring resonators transports fluid to the device and has cross sectional dimensions of 300 microns by 30 microns. The volume to cover the ring resonator is on the order of a few nanoliters, and therefore contains thousands of enzymes. However, the effective sensing volume of the device is much smaller since the squared electric field magnitude, $|\vec{E}|^2$, decays to 1% of its value within ~200 nm (as shown by the gray contour line in Fig. 1b). Changes of absorption in the analyte beyond this contour have minimal effect on the device performance due to a lack of overlap with the field. Multiplying the sensing area within the fluid by the ring circumference we find the effective fluidic sensing volume of the device to be ~100 fL. Since we know the concentration of enzymes used for each fluid preparation, we can determine the average number of enzymes within this sensing volume of the ring resonator. Note that the resonator does not actually detect enzymes, but rather the multitude of absorbing reaction products catalyzed by the enzyme. In Fig. 4 we show the average number of enzymes within the 100 fL effective sensing volume of the ring resonator in a well-mixed sample, or equivalently, the number of enzymes it takes to generate the optical absorption present around the ring resonator. For the various fluid preparations used in the experiment, we show that in principle the device can be used to measure the activity of single enzyme molecules. In order for this sensitivity to be fully realized, the sample volume would need to be reduced to the order of tens of femtoliters which is already within current capabilities of nano reaction chambers [26]. This sensitivity will become important for localized detection of enzyme

#138424 - $15.00 USD Received 18 Nov 2010; revised 23 Dec 2010; accepted 27 Dec 2010; published 5 Jan 2011

reactions in microarray applications, in bacterial metabolism identification and in multiplexed highly parallel nano-ELISA systems.

Conclusion

We have demonstrated the ability to detect chromogenic changes in nanoliter volumes of fluid in an optofluidic device at visible wavelengths. The change in the transmission spectrum of a 100 micron radius ring resonator was used to quantify the optical absorbance of fluids covering the microring with a limit of detection of 0.12 cm^{-1}. The device was used to measure fluid absorbance over the optical density range covered by typical spectrophotometers and is sensitive to the activity of individual enzymes for a 100 fL sample volume. The high sensitivity, low analyte consumption, and miniaturization enable the device to be used for on-chip antibody or antigen detection with ELISA as well as other chromogenic based techniques such as bacteria detection.

Acknowledgements

This material is based on work supported by the IGERT Program of the National Science Foundation under Agreement No. DGE-0654112, administered by the Nanobiotechnology Center at Cornell. This work was performed in part at the Cornell NanoScale Facility, a member of the National Nanotechnology Infrastructure Network, which is supported by the National Science Foundation.

#138424 - $15.00 USD Received 18 Nov 2010; revised 23 Dec 2010; accepted 27 Dec 2010; published 5 Jan 2011